DOI: 10.1002/ejic.201100803

Organochromium Complexes Bearing Noninnocent Diimine Ligands

Kevin A. Kreisel,[a] Glenn P. A. Yap,[a] and Klaus H. Theopold*[a]

Keywords: Chromium complexes / Diimine ligands / N ligands / Alkylation / Insertion

We have prepared several anionic and neutral organochromium complexes featuring noninnocent α-diimine ligands. All neutral and anionic complexes refrain from insertion of the C=N bonds of the diimine ligand into the chromium–carbon bonds, presumably due to the reduced nature of the diimine ligand. However, insertion can be facilitated by one-electron oxidation. Thus, oxidation of [(^{H}**L**^{iPr})CrR(THF)] [^{H}**L**^{iPr} = Ar–N=C(H)–(H)C=N–Ar in which Ar = 2,6-diisopropylphenyl and R = CH_2SiMe_3 or CH_3] with $[(C_5H_5)_2Fe]^+$ presumably forms [(^{H}**L**^{iPr})CrR(THF)]$^+$, which contains a neutral diimine ligand coordinated to Cr^{II}. This cationic complex apparently undergoes immediate insertion of the C=N bond of the diimine ligand into the Cr–alkyl bond, followed by C–H activation of the isopropyl substituent of an N–aryl group on the diimine ligand. DFT calculations confirm that [(^{H}**L**^{iPr})-CrR(THF)]$^+$ contains a neutral innocent diimine ligand that undergoes C=N bond insertion into the Cr–R bond.

Introduction

The recent interest in transition-metal complexes containing redox-active ligands has produced a remarkable number of reports detailing unusual electronic and geometric structures as well as unprecedented reactivity.[1] In most cases, the latter is best rationalized based on an assignment of the most appropriate electronic structure. Work by Wieghardt et al. and others has greatly improved our understanding of the noninnocence of a variety of ligands such as pyridinebis(imines),[2] catechols, 1,2-dioxolenes,[11] and α-diimines (also known as diazadienes).[3] Among the most frequently used of these ligands are the α-diimines, due to the ease of varying the sterics and electronics of these ligands. Pioneering work by van Koten showed the diversity in the reactivity of diimine ligands and established the potential noninnocence of the ligand by means of radical C–C coupling reactions between coordinated diimine ligands.[4] Arguably more interesting and perhaps mechanistically related to our work was the discovery of regioselective alkylation of diimine ligands by diorganozinc reagents.[5] Since then, the reactions of diimines with organozinc, organomagnesium, and organoaluminum reagents have been studied extensively.[5b,6] In many cases, these reactions lead to alkylation of the diimine ligand at various positions (see Scheme 1). More recently, there have been reports of transition metals mediating the alkylation of diimine ligands. Most relevant to our work are reports of the reactions of zirconium- and hafnium-alkyl compounds with diimine ligands and their use as catalysts in olefin polymerization.[7] Thus, the reaction of $M(CH_2Ph)_4$ (M = Zr or Hf) with *N*-aryl-substituted diimine ligands results in alkyl migration to the carbon atom of the diimine ligand and a 1,2-hydride shift, thereby leaving an amido–imine ligand coordinated to the metal. However, the mechanism of this rearrangement is still not entirely clear.

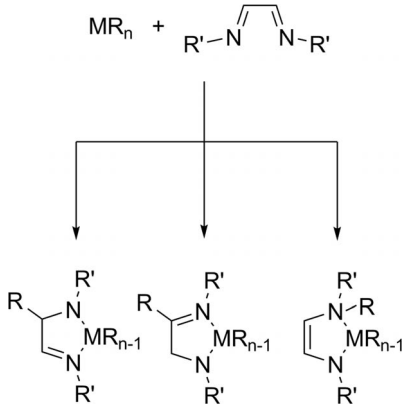

Scheme 1. Possible regioisomers produced by alkylation of a diimine ligand.

We recently reported a thorough investigation of the coordination chemistry of chromium-bearing diimine ligands utilizing both X-ray crystallography and density functional theory (DFT) calculations;[8] the present work extends this work to organometallic derivatives. An understanding of the electronic structure of these complexes facilitates a rationalization of their reactivity. Furthermore, the results presented here provide insight into the mechanism of alkyl

[a] Department of Chemistry and Biochemistry,
Center for Catalytic Science and Technology,
University of Delaware,
Newark, Delaware 19716, USA
Fax: +1-302-831-6335
E-mail: theopold@udel.edu

Supporting information for this article is available on the WWW under http://dx.doi.org/10.1002/ejic.201100803 or from the author.

migrations that have plagued organometallic diimine chemistry for decades.

Herein, we summarize our study of the organometallic chemistry of chromium supported by the diimine ligand, Ar–N=C(H)–(H)C=N–Ar ($^{H}L^{iPr}$; Ar = 2,6-diisopropylphenyl). The original intent of this work – in the context of Phillips catalysis of ethylene polymerization[9] – was to prepare cationic Cr^{II}-monoalkyls supported by bidentate nitrogen ligands, and to compare their catalytic activity for ethylene polymerization to alkyl-Cr^{III} compounds.[10] Although this goal was not realized, the results of our study shed light on a characteristic reaction pattern of diimine metal–alkyl complexes.

Results and Discussion

Our initial attempts to prepare dialkyl-Cr^{II} complexes of the type [($^{H}L^{iPr}$)CrR_2] by the reaction of [{($^{H}L^{iPr}$)Cr(μ-Cl)(Cl)}$_2$] with four equivalents of alkylating agents, such as PhMgCl or $(Me)_3SiCH_2Li$, indeed gave novel organometallic compounds, but in low yield. Full characterization of the reaction products revealed them to be formally Cr^{I}–dialkyl "ate" complexes of the general formula [($^{H}L^{iPr}$)-CrR_2]$^-$. Seeking to circumvent the apparent reduction of chromium by the electron-rich main-group alkyls, we eventually prepared the precursor [{($^{H}L^{iPr}$)Cr(μ-Cl)}$_2$] (**1**). As discussed elsewhere, the latter is best described as containing divalent chromium (Cr^{II}), coordinated by a singly reduced α-diimine radical anion.[8] Compound **1** is also an easily accessible synthon for the preparation of the aforementioned dialkyls in good yield (see Scheme 2). Upon addition of alkylating reagent (4 equiv.), excellent yields of [$Li(THF)_4$][($^{H}L^{iPr}$)Cr{$CH_2Si(CH_3)_3$}$_2$] (**2**) and [PhMg(THF)][($^{H}L^{iPr}$)$CrPh_2$] (**3a**) or [$Li(THF)_2$][($^{H}L^{iPr}$)$CrPh_2$] (**3b**) could be obtained. The molecular structures of **2** and **3a** were determined by X-ray crystallographic analysis; the molecular structures are depicted in Figures 1 and 2, respectively. Complex **2** crystallizes in the monoclinic space group $P2_1/n$ and displays a significantly distorted square-planar geometry. Its Cr–C bond lengths of 2.131(5) and 2.136(5) Å are in good agreement with other reported alkyl complexes of chromium. The Cr–N bond lengths of 1.994(4) and 2.004(4) Å are also similar to those of previously reported chromium diimine complexes. In addition, the THF-solvated lithium cation shows no signs of interaction with the chromate anion in the solid state [closest contact distance is 3.506(11) Å]. The phenyl derivative **3a** crystallizes in the monoclinic space group $P2_1/c$ and also exhibits distorted square-planar coordination geometry about chromium. The Cr–C bond lengths in **3a**, at 2.164(2) and 2.203(2) Å, are longer than those in **2**, presumably reflecting the pronounced bonding interaction of the phenyl groups with the magnesium counterion. The Cr–N bond lengths are also slightly elongated [2.0362(19) and 2.0613(19) Å]. The cation in **3a** {i.e., [PhMg(THF)]$^+$} is positioned close to the *ipso*-carbon atoms of both phenyl groups of the organochromium complex ion. When prepared from PhLi (see

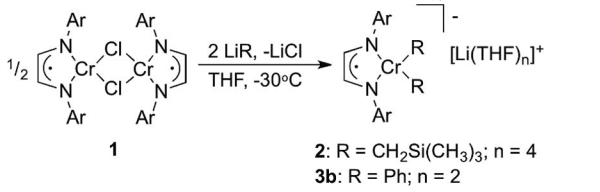

Scheme 2. Synthesis of complexes **2** and **3**.

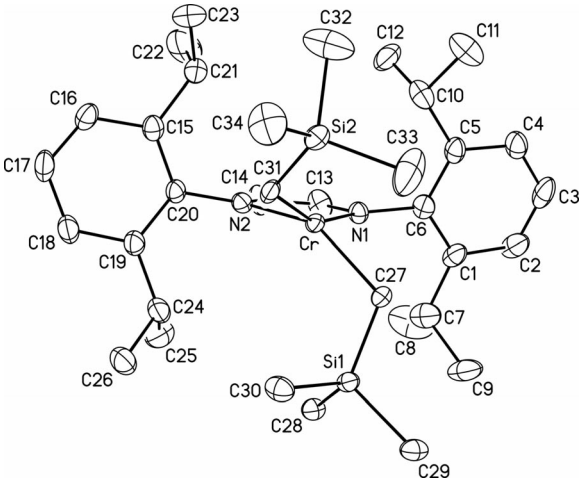

Figure 1. ORTEP plot of [$Li(THF)_4$][($^{H}L^{iPr}$)Cr{$CH_2Si(CH_3)_3$}$_2$] (**2**) at the 30% probability level. Hydrogen atoms and the $[Li(THF)_4]^+$ cation have been omitted for clarity. Selected structural parameters (distances in Å, angles in degrees): Cr–N1 2.004(4), Cr–N2 1.993(4), Cr–C27 2.131(5), Cr–C31 2.136(5), N1–C13 1.335(7), N2–C14 1.352(6), C13–C14 1.372(8); N1–Cr–N2 79.27(16), N1–Cr–C27 96.60(18), N1–Cr–C31 156.87(18), N2–Cr–C27 148.69(18), N2–Cr–C31 97.93(17), C27–Cr–C31 97.22(19).

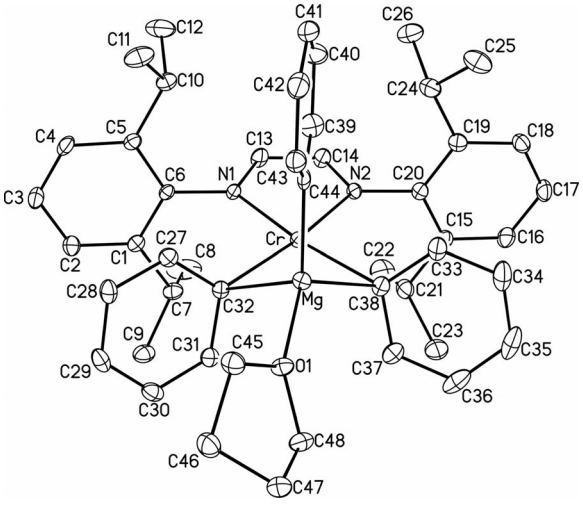

Figure 2. ORTEP plot of [PhMg(THF)][($^{H}L^{iPr}$)$CrPh_2$] (**3a**) at the 30% probability level. Hydrogen atoms have been omitted for clarity. Selected structural parameters (distances in Å, angles in degrees): Cr–N1 2.0362(19), Cr–N2 2.0613(19), Cr–C32 2.164(2), Cr–C38 2.203(2), N1–C13 1.335(3), N2–C14 1.335(3), C13–C14 1.383(3); N1–Cr–N2 78.61(8), N1–Cr–C32 92.21(8), N1–Cr–N38 172.45(8), N2–Cr–C32 170.54(8), N2–Cr–C38 94.01(8), C32–Cr–C38 95.23(9).

Scheme 2), we assume that the lithium cation of **3b** also lies between the aryl rings and is coordinated by two THF ligands; this assertion is consistent with the elemental analysis (see the Exp. Section). X-ray quality crystals of **3b** were not attainable; however, the reaction was cleaner and resulted in higher yields. The diimine backbones of both **2** and **3a** show signs of reduction, consistent with one-electron reduced ligand-centered radicals.[8] Considering these bond lengths and the square-planar coordination favored by divalent chromium, the most appropriate assignment of an electronic structure to these complexes would be Cr^{II} (d^4, $S = 2$) with strong antiferromagnetic coupling to a ligand-centered radical, analogous to $[(^{H}\mathbf{L}^{i\mathrm{Pr}})CrCl_2]^-$ ($S = {}^3/_2$). Accordingly, room-temperature measurements of the effective magnetic moments (μ_{eff}) of **2** and **3b** gave 3.7(1) μ_B for both complexes, close to the spin-only moment for three unpaired electrons (3.87 μ_B).[11]

Interestingly, alkylation of **1** with MeLi (4 equiv.) did not give the expected $[Li(THF)_4][(^{H}\mathbf{L}^{i\mathrm{Pr}})Cr(CH_3)_2]$, but instead yielded dinuclear $[Li(THF)_4][\{(^{H}\mathbf{L}^{i\mathrm{Pr}})Cr\}_2(\mu\text{-}CH_3)_3]$ (**4**). In a similar manner, the reaction of **1** with an excess amount of $Li[BEt_3H]$ gave $[Li(THF)_4][\{(^{H}\mathbf{L}^{i\mathrm{Pr}})Cr\}_2(\mu\text{-}H)_3]$ (**5**), which is isostructural to **4**. Both **4** and **5** could also be prepared in good yield by addition of three equivalents of the appropriate alkylating reagent to **1** according to Scheme 3. Crystallizations from Et_2O at –30 °C gave blue crystals of **4** and purple crystals of **5**, respectively. The molecular structures of **4** and **5** are shown in Figures 3 and 4, respectively, along with selected interatomic distances and angles. Complex **4** crystallizes in the monoclinic space group $P2_1/c$ and contains two diimine chromium fragments joined by three bridging methyl ligands. The coordination geometry about each chromium atom is best described as trigonal bipyramidal, with the threefold axes approximated by C3–Cr1–N1 [168.23(16)°] and C1–Cr2–N3 [157.77(16)°]. The Cr–C distances range from 2.176(5) to 2.243(5) Å and are thus longer than those in the monomeric complexes described above, presumably due to three-center two-electron bonding. The bridging methyl ligands also fix the chromium atoms at a metal–metal distance of 2.469(1) Å, raising the possibility of metal–metal bonding. Indeed, the $[Cr_2(\mu\text{-}CH_3)_3]$ core of **4** is remarkably similar in structure to that of $[Cp^*_2Cr_2(\mu\text{-}CH_3)_3]BF_4$ (e.g., Cr–Cr 2.42 Å; Cp* = pentamethylcyclopentadienyl), to which we have attributed metal–metal bonding between its Cr^{III} centers many years ago.[12] The Cr–N distances in **4** [1.988(3) to 2.006(4) Å] are consistent with those in **1**. The THF-solvated lithium cation does not exhibit any close contacts with the anion; the closest internuclear distance between the two measures is 3.843(9) Å. The isostructural complex **5** crystallizes in the triclinic space group $P\bar{1}$, with each chromium also residing in a trigonal-bipyramidal coordination sphere – the axial vectors being defined by H1C–Cr1–N2 [168.8(9)°] and H1C–Cr2–N4 [168.8(9)°]. Although there is always a systematic error involved with hydride bond lengths established by X-ray crystallography,[13] the apparent Cr–H distances for the bridging hydride ligands range from 1.61(3)–1.78(3) Å and are comparable to other reported bridging hydrides of chromium.[14] The Cr–Cr distance of **5** is similar, although slightly shorter than that of **4**, measuring 2.4490(7) Å. The Cr–N distances in **5** are considerably shorter than in the previously mentioned complexes [1.952(2) to 1.957(2) Å]. Similar to **4**, the countercation of **5** is not closely associated with the chromate anion, with a distance of 3.594(5) Å between them. Both **4** and **5** show considerable disruption of the diimine π system and, based solely on bond lengths (**4**: $C–N_{av.}$ 1.375 Å; $C–C_{av.}$ 1.355 Å; **5**: $C–N_{av.}$ 1.371 Å; $C–C_{av.}$ 1.352 Å), the ligands appear to be closest to the dianionic enediamide electronic configuration. The latter would result in the assignment of +III as a formal oxidation state of chromium. Room-temperature magnetic measurements of **4** and **5** gave μ_{eff} values of 1.4(1) and 1.5(1) μ_B per Cr, respectively. These low values (the ex-

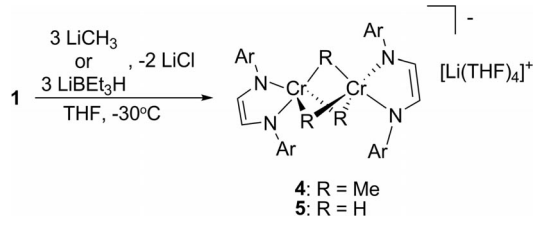

Scheme 3. Synthesis of bridging alkyl species **4** and **5**.

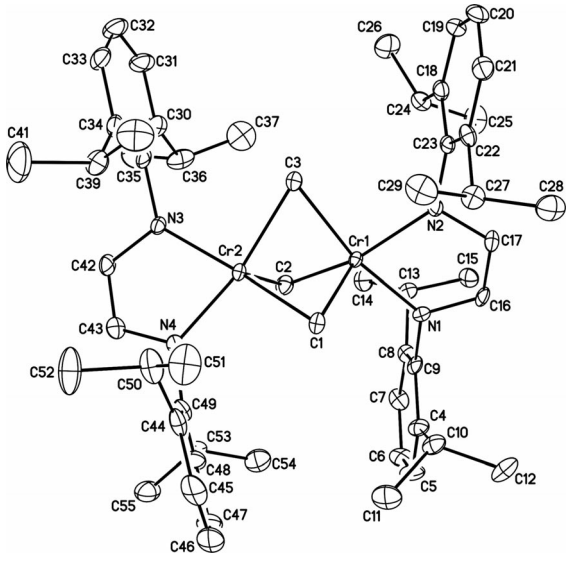

Figure 3. ORTEP plot of $[Li(THF)_4][\{(^{H}\mathbf{L}^{i\mathrm{Pr}})Cr\}_2(\mu\text{-}CH_3)_3]$ (**4**) at the 30% probability level. Hydrogen atoms and the $[Li(THF)_4]^+$ cation have been omitted for clarity. Selected structural parameters (distances in Å, angles in degrees): Cr1–Cr2 2.4690(10), Cr1–N1 2.006(4), Cr1–N2 2.002(3), Cr1–C1 2.192(4), Cr1–C2 2.235(5), Cr1–C3 2.202(5), Cr2–N3 1.990(4), Cr2–N4 1.988(3), Cr2–C1 2.243(5), Cr2–C2 2.176(5), Cr2–C3 2.221(5), N1–C16 1.366(6), N2–C17 1.393(6), N3–C42 1.367(5), N4–C43 1.374(6), C16–C17 1.349(6), C42–C43 1.361(7); Cr1–C1–Cr2 67.65(13), Cr1–C2–Cr2 68.07(14), Cr1–C3–Cr2 67.87(15), N1–Cr1–N2 79.51(14), N1–Cr1–C1 102.91(16), N1–Cr1–C2 93.16(17), N1–Cr1–C3 168.23(16), N2–Cr1–C1 116.96(17), N2–Cr1–C2 146.72(16), N2–Cr1–C3 90.37(16), N3–Cr2–N4 79.69(15), N3–Cr2–C1 157.77(16), N3–Cr2–C2 105.70(18), N3–Cr2–C3 93.41(16), N4–Cr2–C1 94.06(16), N4–Cr2–C2 106.69(17), N4–Cr2–C3 160.06(17).

pected spin-only value for $S = {}^3/_2$ is 3.88 μ_B) are consistent with antiferromagnetic coupling between the chromium ions, metal–metal bonding, or a combination of the two.

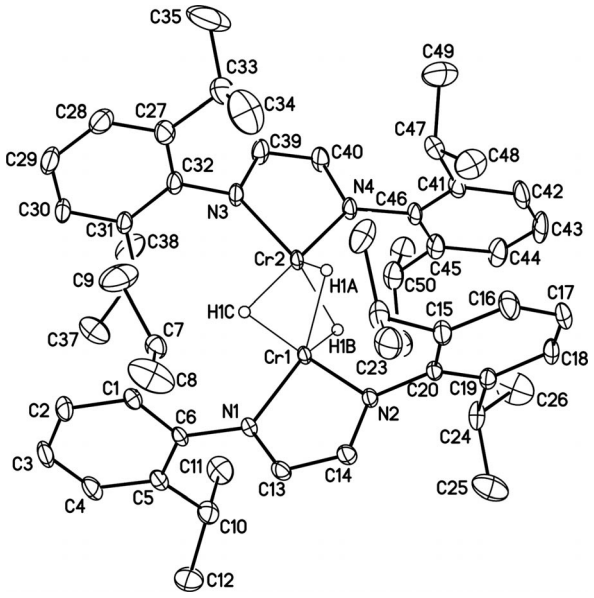

Figure 4. ORTEP plot of $[Li(THF)_4][\{(^HL^{iPr})Cr\}_2(\mu\text{-}H)_3]$ (**5**) at the 30% probability level. With the exception of the bridging hydride ligands, all hydrogen atoms and the $[Li(THF)_4]^+$ cation have been omitted for clarity. Selected structural parameters (distances in Å, angles in degrees): Cr1–Cr2 2.4490(7), Cr1–N1 1.9544(18), Cr1–N2 1.9524(19), Cr1–H1A 1.78(3), Cr1–H1B 1.72(3), Cr1–H1C 1.71(3), Cr2–N3 1.957(2), Cr2–N4 1.955(2), Cr2–H1A 1.61(3), Cr2–H1B 1.69(3), Cr2–H1C 1.68(3), N1–C13 1.374(3), N2–C14 1.372(3), N3–C39 1.3733, N4–C40 1.366(3), C13–C14 1.349(3) C39–C40 1.355(4); Cr1–H1A–Cr2 92.3(9), Cr1–H1B–Cr2 91.8(9), Cr1–H1C–Cr2 92.3(9), N1–Cr1–N2 80.42(8), N1–Cr1–H1A 147.5(9), N1–Cr1–H1B 141.0(9), N1–Cr1–H1C 97.9(9), N2–Cr1–H1A 103.5(9), N2–Cr1–H1B 112.7(9), N2–Cr1–H1C 168.8(9), N3–Cr2–N4 80.56(9), N3–Cr2–H1A 124.7(9), N3–Cr2–H1B 160.7(9), N3–Cr2–H1C 97.1(9), N4–Cr2–H1A 113.1(9), N4–Cr2–H1B 101.3(9), N4–Cr2–H1C 168.8(9).

Reaction of **1** with an excess amount of $LiCH_3$ resulted in the formation of a red product that was ultimately determined to be $[Li_2(THF)_3][(^HL^{iPr})Cr(CH_3)_3]$ (**6**) by X-ray crystallography (see Scheme 4). Interestingly, reaction of **1** with an excess amount of $Li[BEt_3H]$ only gave **5** in low yield; $[Li_2(THF)_3][(^HL^{iPr})CrH_3]$ was not isolated. Figure 5 depicts the results of the X-ray structure determination of **6**.

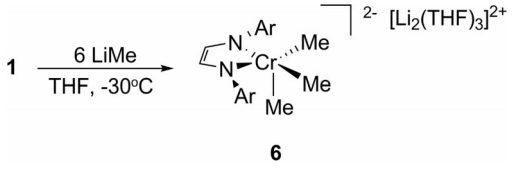

Scheme 4. Preparation of $[Li_2(THF)_3][(^HL^{iPr})Cr(CH_3)_3]$ (**6**).

The trialkyl crystallizes in the monoclinic space group *C*2/*c*. The geometry about the chromium in **6** is best described as square pyramidal with the angles between the apical ligand (C29) and the basal ones ranging from 91.2(2) to 103.9(1)°. The Cr–C distances [2.107(4), 2.150(5), and

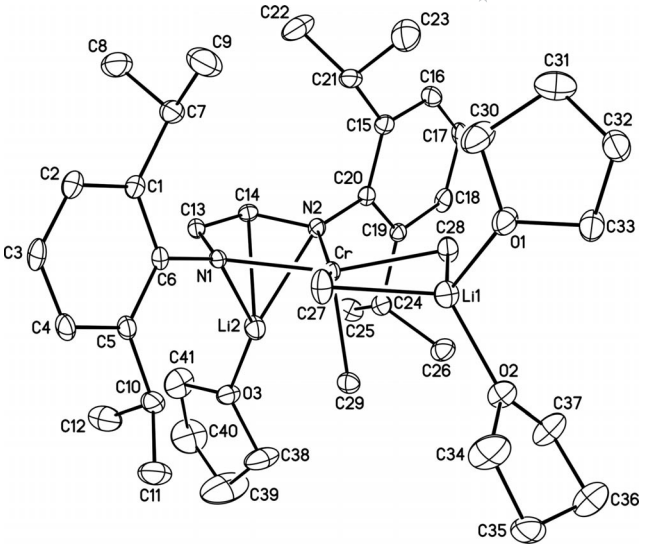

Figure 5. ORTEP plot of $[Li_2(THF)_3][(^HL^{iPr})Cr(CH_3)_3]$ (**6**) at the 30% probability level. Hydrogen atoms have been omitted for clarity. Selected structural parameters (distances in Å, angles in degrees): Cr–N1 2.081(3), Cr–N2 2.066(3), Cr–C27 2.159(5), Cr–C28 2.150(5), Cr–C29 2.107(4), N1–C13 1.402(4), N2–C14 1.401(4), C13–C14 1.344(5); N1–Cr–N2 76.7(1), N1–Cr–C27 89.7(2), N1–Cr–C28 161.7(2), N1–Cr–C29 103.9(1), N2–Cr–C27 159.1(2), N2–Cr–C28 90.2(2), N2–Cr–C29 102.6(2), C27–Cr–C28 99.0(2), C27–Cr–C29 96.0(2).

2.159(5) Å] are shorter than in the dinuclear complex **4** and more closely approximate the Cr–C bond lengths in **2** and **3**. Notably, the two lithium cations in **6** are closely associated with the chromate anion; one interacts with the two equatorial methyl ligands and the other is coordinated in a η^4 fashion by the reduced diimine ligand. This diimine coordination of the cation is rare, but some examples do exist.[15] Like complexes **4** and **5**, the C–N distances of 1.401(4) and 1.402(4) Å and the C–C distance of 1.344(5) Å are in accord with a heavily reduced diimine ligand, most likely to the extent of a dianionic, enediamide ligand. A magnetic susceptibility measurement of **6** gave a μ_{eff} of 3.8(1) μ_B, in accord with an $S = {}^3/_2$, Cr^{III} bound to a diamagnetic enediamide ligand.

Condensation of alkyl complexes **2**, **4**, and **6** with **1** in the proper stoichiometry readily furnishes neutral, monoalkyl complexes. Thus, reaction of two equivalents of **2** with **1** gives $[(^HL^{iPr})Cr\{CH_2Si(CH_3)_3\}(THF)]$ (**7**) in good yield (see Scheme 5). The results of an X-ray structure determination can be found in Figure 6.

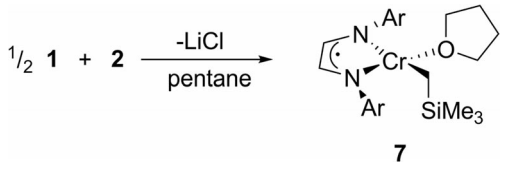

Scheme 5. Preparation of $[(^HL^{iPr})Cr\{CH_2Si(CH_3)_3\}(THF)]$ (**7**).

Complex **7** crystallizes in the monoclinic space group $P2_1/n$ with two crystallographically distinct, but chemically equivalent molecules (only one will be discussed). The dis-

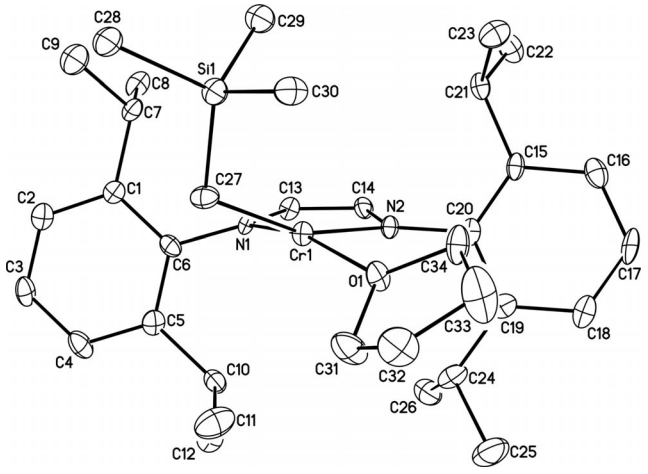

Figure 6. ORTEP plot of [(^{H}L^{iPr})Cr{$CH_2Si(CH_3)_3$}(THF)] (**7**) at the 30% probability level. Hydrogen atoms have been omitted for clarity. Selected structural parameters (distances in Å, angles in degrees): Cr1–N1 1.993(4), Cr1–N2 2.034(4), Cr1–C27 2.102(5), Cr1–O1 2.104(4), N1–C13 1.338(6), N2–C14 1.347(6), C13–C14 1.376(7); N1–Cr1–N2 78.90(18), N1–Cr1–C27 96.6(2), N1–Cr1–O1 164.59(16), N2–Cr1–C27 160.3(2), N2–Cr1–O1 95.26(16), C27–Cr1–O1 93.5(2).

torted square-planar geometry around the Cr in **7** is similar to that of its precursor, **2**. However, the Cr–C bond length of 2.098(6) Å is shorter than those in **2**, presumably due to the relief of the anionic charge buildup on the complex. The difference in the Cr–N distances of 1.995(5) Å (Cr–N1) and 2.035(5) Å (Cr–N2) can be attributed to a *trans* influence imparted by the alkyl group that is *trans* to N2. Like **2**, the reduction of the diimine ligand in **7** can be seen through the C–N bond lengths of 1.336(6) and 1.344(6) Å and the C–C bond length of 1.373(7) Å. This, and the room-temperature magnetic moment of 3.8(1) μ_B, are consistent with a $S = 2$, Cr^{II} complex strongly antiferromagnetically coupled to a ligand-centered radical.

In a similar manner, condensation of **1** with complex **4** or **6** in the proper stoichiometry yields the neutral, methyl-bridged dimer, [{(^{H}L^{iPr})Cr(μ-CH_3)}$_2$] (**8**) according to Scheme 6. The results of an X-ray analysis of **8** can be found in Figure 7.

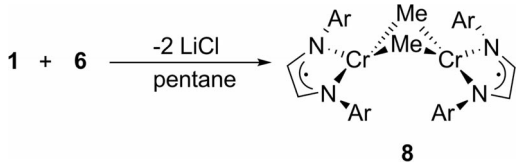

8

Scheme 6. Preparation of [{(^{H}L^{iPr})Cr(μ-CH_3)}$_2$] (**8**).

Complex **8** crystallizes in the monoclinic space group *C*2/*c* with a C_2 axis running perpendicular to the Cr–Cr vector and between the bridging methyl ligands. The geometry around each chromium atom is best described as distorted square planar with a dihedral angle of 20.1° between the N1–Cr1–N2 plane and the C1–Cr1–C1A plane. The two diimine chromium fragments are "folded" toward each other at the bridging methyl ligands at an angle of 53.0°

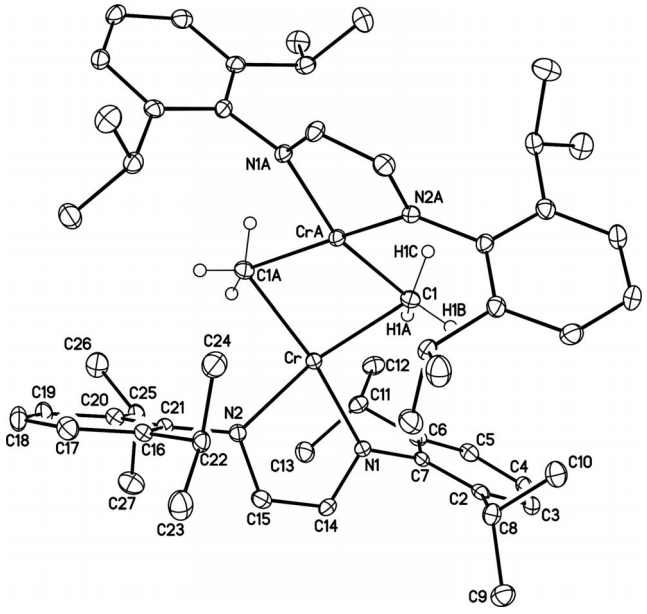

Figure 7. ORTEP plot of [{(^{H}L^{iPr})Cr(μ-CH_3)}$_2$] (**8**) at the 30% probability level. With the exception of the hydrogen atoms on the methyl ligands, all hydrogen atoms have been omitted for clarity. Selected structural parameters (distances in Å, angles in degrees): Cr–CrA 2.6649(8), Cr–N1 2.043(2), Cr–N2 2.026(2), Cr–C1 2.192(3), Cr–C1A 2.197(3), N1–C14 1.347(3), N2–C15 1.347(3), C14–C15 1.377(3); N1–Cr–N2 79.6(1), N1–Cr–C1 163.9(1), N1–Cr–C1A 93.6(1), N2–Cr–C1 95.3(1), N2–Cr–C1A 164.1(1), C1–Cr1–C1A 95.0(1).

(see Figure 7), which is likely due to some measure of Cr–Cr bonding, supported by the short metal–metal distance [Cr–Cr 2.6649(8) Å].[14d] The methyl ligands are symmetrically bridged with bond lengths of 2.192(3) and 2.197(3) Å. As in **4**, these long Cr–C distances are presumably a consequence of three-center two-electron bonding. Complex **8** has average C–N bond lengths of 1.347(3) Å and a diimine C–C bond length of 1.377(3) Å, making it most consistent with a high-spin Cr^{II} complex ($S = 2$) coupled to a ligand-centered radical. The room-temperature effective magnetic moment [1.8(1) μ_B per Cr] indicates appreciable metal–metal interactions, either Cr–Cr bonding or antiferromagnetic coupling or more likely a combination of both, much like in **4** and **5**. The solution behavior of **8** in C_6D_6 is in accord with the solid-state structure shown in Figure 7, with a very broad, isotropically shifted resonance at δ = 17.4 ppm and sharp resonances at δ = 8.49, 3.88, and 1.64 ppm in the ^{1}H NMR spectra. In [D_8]THF a dramatically different spectrum is obtained; thus, the broad resonance is shifted to –13.1 ppm while the others are located at 14.4, 2.69, and –1.91 ppm. We attribute these spectral differences to the formation of mononuclear [(^{H}L^{iPr})-Cr(Me)(THF)] in THF solution. The ^{1}H NMR spectrum of **8** in [D_8]THF is similar in appearance to that of its presumed analogue, complex **7** (see Exp. Section). A reaction of **5** with **1** was also attempted to generate a hydride species similar to **8**, namely, [{(^{H}L^{iPr})Cr(μ-H)}$_2$]. However, we found that the stronger Cr–H bonds in **5** would not give way as the Cr–C bonds in **4** and **6** had done. Other methods

of generating [{(^{H}**L**$^{i\mathrm{Pr}}$)Cr(μ-H)}$_2$] from **1** (e.g., $AlEt_2Cl$, through β-hydrogen elimnation of an ethyl intermediate) produced a brown material with ^{1}H NMR spectroscopic resonances at 21.0, 2.17, 8.72, and –24.3 ppm. However, the reaction consistently produced intractable materials and structural characterization of the product was not achievable in this context {note, however, the initial isolation of [{(^{H}**L**$^{i\mathrm{Pr}}$)Cr}$_2$] from a related reaction}.[16]

With neutral alkyl complexes **7** and **8** in hand, oxidation was attempted to generate cationic alkylchromium complexes. Cr^{III} complexes of this type have proved to be very successful homogeneous ethylene polymerization catalysts.[10] However, oxidation of **7** with [$(C_5H_5)_2$Fe][BARF] [BARF = tetrakis(3,5-bis(trifluoromethyl)phenyl)borate] in Et_2O, intended to produce the cationic, formally Cr^{II} complex, [(^{H}**L**$^{i\mathrm{Pr}}$)Cr(CH_2SiMe_3)(THF)]$^+$, instead led to the product of a tortuous alkyl/hydride migration and C–H activation (see Scheme 7).

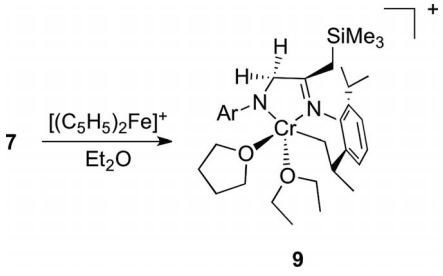

Scheme 7. Preparation of [(^{H,TMSM}**L***)Cr(THF)(Et_2O)][BARF] (**9**).

The ionic product isolated from the oxidation reaction, brown [(^{H,TMSM}**L***)Cr(THF)(Et_2O)][BARF] (**9**, in which ^{H,TMSM}**L** denotes alkyl migration to the backbone of what is now an iminoylamide ligand and **L*** denotes C–H activation of an isopropyl methyl group of an aryl substituent), crystallized in the triclinic space group $P\bar{1}$; the result of the structure determination is depicted in Figure 8. The structure of **9** is best described as square pyramidal with apical (C30) to basal bond angles ranging from 86.7(3) to 117.1(2)°. The Cr–C bond length is 2.053(6) Å and is thus consistent with typical Cr^{III}–C bond lengths. More interesting, however, is the apparent migration of the (trimethylsilyl)methyl group to the backbone of the diimine ligand. Close inspection of the bond lengths shows that the N1–C13 and C13–C14 bond lengths have lengthened to 1.451(8) and 1.480(9) Å, respectively, whereas the N2–C14 bond length is considerably shorter [1.306(7) Å] than the bond lengths in the precursor, complex **7**. Furthermore, the IR spectrum of **9** shows the appearance of a band at 1610 cm^{-1} consistent with a C=N vibration. These observations would suggest that the backbone of the ligand is in an imine–amide form with one C–N double bond, one C–N single bond, and a C–C single bond. Thus, the oxidation state ambiguity in the previous complexes has been removed and straightforward electron counting reveals a 13-electron, d^3, Cr^{III} complex ion. Accordingly, the experimentally determined magnetic moment was found to be 4.0(1) μ_B, consistent with the $S = {}^3/_2$ spin state of a typical Cr^{III} compound. Oxidation of the methyl-bridged **8** in THF also gave a brown solution that was proposed to be [(^{H,Me}**L***)Cr(THF)$_2$][BARF] (**10**) and has a similar ^{1}H NMR spectrum to that of **9** (see the Exp. Section).

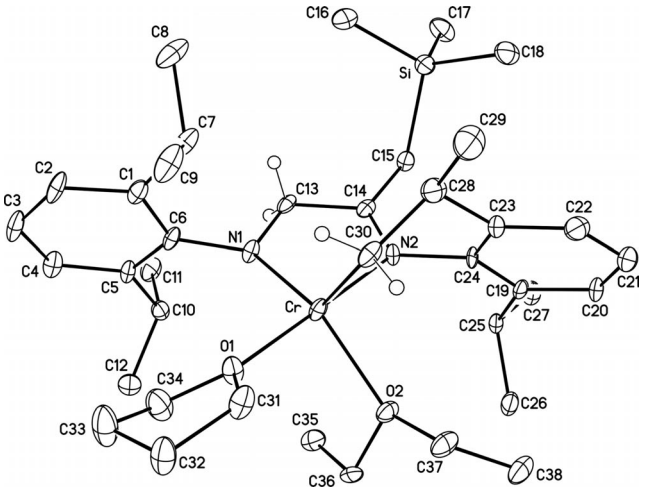

Figure 8. ORTEP plot of [(^{H,TMSM}**L***)Cr(THF)(Et_2O)][BARF] (**9**) at the 30% probability level. With the exception of the hydrogen atoms on C13 and C30, all hydrogen atoms and the [BARF]$^-$ anion have been omitted for clarity. Selected structural parameters (distances in Å, angles in degrees): Cr–N1 1.920(4), Cr–N2 2.013(5), Cr–C30 2.053(6), Cr–O1 2.065(4), Cr–O2 2.144(4), N1–C13 1.454(8), N2–C14 1.308(7), C13–C14 1.486(8), C14–C15 1.493(7); N1–Cr–N2 81.7(2), N1–Cr–C30 117.2(2), N1–Cr–O1 96.74(18), N1–Cr–O2 145.41(18), N2–Cr–C30 86.6(2), N2–Cr–O1 177.90(19), N2–Cr–O2 92.56(18), O1–Cr–O2 87.95(16), O1–Cr–C30 95.3(2), O2–Cr–C30 96.3(2).

Two mechanisms have been proposed for alkyl migration to C=N bonds in diimine ligands. The first involves homolytic cleavage of the metal–alkyl bond followed by recombination of the alkyl radical with a diimine ligand-centered radical. The second mechanism assumes 1,2-insertion of a C=N bond of the diimine ligand into a metal–alkyl bond. Either reaction step is then followed by a 1,2-hydride shift to engender unsaturation at the more substituted C–N bond. Assuming the HOMO of **7** houses the ligand-centered unpaired electron, oxidation would presumably produce [(^{H}**L**$^{i\mathrm{Pr}}$)Cr(CH_2SiMe_3)(THF)]$^+$, which contains a neutral diimine ligand and Cr^{II} (see Scheme 8). This intermediate could undergo either a 1,2-insertion of the alkyl ligand into the C–N double bond or homolytic cleavage of the alkyl and single-electron transfer to the diimine ligand, followed by radical recombination. Either of these steps is then followed by a hydride shift to the remaining imine carbon and reestablishment of the C–N double bond at the bulkier, alkyl-substituted side of the ligand. The resulting cationic Cr^{II} complex activates a C–H bond of an isopropyl substituent and a bimolecular reductive elimination of H_2 finally furnishes **9**. The C–H bond-activation step is an apparent consequence of the formation of a highly reactive, three-coordinate, cationic, Cr^{II} species.

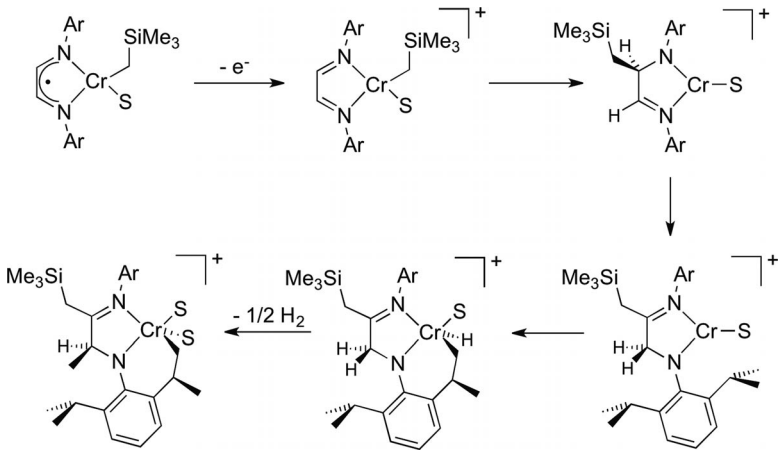

Scheme 8. Mechanism of formation of oxidation product **9** (S = THF, Et_2O).

For a better understanding of the relative propensity of metal alkyls such as **7** or its oxidized form towards alkyl migration, unrestricted DFT calculations at the B3LYP/6-311g level of theory were run on model complexes [(^{H}**L**^{Me})-Cr(Me)(THF)] (**7′**), [(^{H,Me}**L**^{Me})Cr(THF)] (**7′′**), [(^{H}**L**^{Me})-Cr(Me)(THF)]$^+$ (**8′**), and [(^{H,Me}**L**^{Me})Cr(THF)]$^+$ (**8′′**), in which the 2,6-diisopropylphenyl substituents and the alkyl ligand have all been replaced by methyl groups. A geometry optimization of **7′** gave metric parameters that are in excellent agreement (ΔC–N $<$ 0.020 Å; ΔC–C $\leq$ 0.022 Å; ΔCr–N $\leq$ 0.048 Å, ΔCr–C = 0.035 Å, ΔCr–O = 0.020 Å) with those of actual **7**, and its electronic structure is consistent with our assignment that chromium is in the +II oxidation state and the diimine ligand is reduced to a ligand-centered radical resulting in a $S = {}^3/_2$ ground state (see the Supporting Information).

An alkyl migration and subsequent hydride shift in **7′** would furnish **7′′** (see Figure 9). Single-point calculations of geometry-optimized structures of the $S = {}^5/_2$, ${}^3/_2$, and ${}^1/_2$ spin-state possibilities for **7′′** showed the quartet ($S = {}^3/_2$) to be most stable. Complex ^{4}**7′′** shows ligand bond lengths that are in accord with an iminoamide-type structure with unsaturation at the alkyl-substituted carbon position. Not only does this formulation result in an apparent reduction of the metal to Cr^{I}, a relatively unstable oxidation state for Cr, but most importantly, ^{4}**7′′** is calculated to be approximately 42 kcal mol^{-1} less stable than **7′**. In silico oxidation of **7′** to **8′** results in oxidation of the ligand-centered radical and formation of a high-spin diimine complex of Cr^{II} (d^4, $S = 2$). This spin state was found to be lower in energy than the corresponding triplet and singlet states. Complex ^{5}**8′** has bond lengths that are in accord with a neutral diimine ligand, that is, C–N distances of 1.2986 and 1.2964 Å and a C–C distance of 1.4617 Å. Furthermore, the Cr–O_{THF} and Cr–CH_3 bond lengths are shorter than those in **7′** due to the increase in formal charge on Cr. The calculation on the migratory insertion product of **8′**, namely **8′′**, produced metric parameters for the diimine ligand that are essentially identical to those in **7′′**; thus the ligand is clearly an iminoamide ligand. Like **8′**, complex **8′′** is also calculated to be a quintet ($S = 2$) Cr^{II} complex, this spin state being lower in energy than the $S = 1$ and $S = 0$ spin states. Unlike the **7′** to **7′′** rearrangement, the **8′** to **8′′** transformation is calculated to be energetically favorable by approximately 10 kcal mol^{-1}. These calculations are wholly consistent with our experimental observations, and they suggest that cationic alkyl-Cr^{II} complexes are subject to facile migratory insertions of unsaturated molecules into the chromium–carbon bond, at least in an intramolecular fashion.

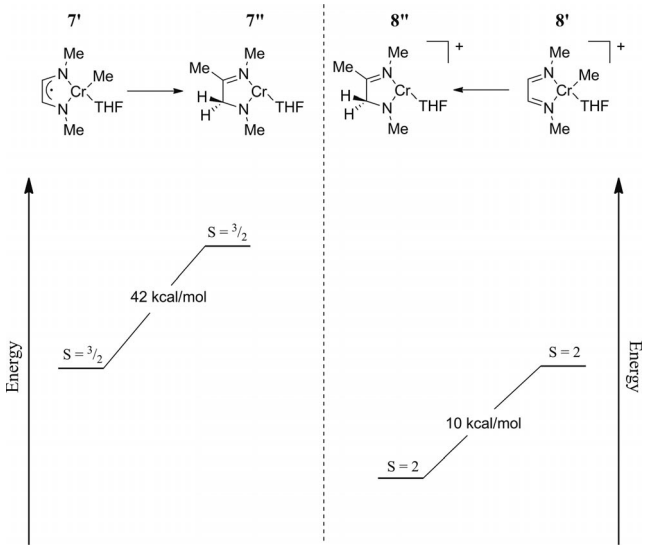

Figure 9. Relevant energies (not to scale), structures, and spin states for model complexes **7′**, **7′′**, **8′**, and **8′′**.

Conclusion

Several open-shell organometallic derivatives of chromium supported by a redox noninnocent diimine ligand have been prepared. These compounds feature reduced diimine ligands, with the extent of electron transfer depending on the particular compound. As the metal – which is only formally in the Cr^{I} oxidation state – finds itself in a more

and more electron-rich coordination environment (i.e., the more alkyl ligands it has and the more negatively charged it is), the diimine radical anion accommodates the extra electron density to the point where it oxidizes even Cr^{II}, resulting in a formal Cr^{III}/enediamide pairing. Furthermore, we have shown that alkyl chromate and neutral organochromium complexes resist alkyl migration to the ligand, perhaps due to the reduced nature of the latter. However, upon oxidation to cationic alkyls, which feature neutral diimine ligands, migratory insertion of the C=N double bond into the metal–carbon bond becomes favorable and indeed facile. This suggests that organometallic diimine complexes of early transition metals will be most stable in the presence of appreciably reduced diimine ligands.

While α-diimines make excellent ancillary ligands for homogeneous olefin polymerization catalysts containing late-transition metals,[17] we anticipate that they will be less than "ancillary" when coordinated to metals on the left side of the periodic table.

Experimental Section

General: All manipulations were carried out with standard Schlenk, vacuum line, and glovebox techniques. Pentane, diethyl ether, and tetrahydrofuran were dried by passing the solvent through a column of activated alumina and sparging with N_2 to remove residual O_2 prior to use. [D_8]THF was predried with potassium metal and stored under vacuum over Na/K. C_6D_6 was predried with sodium metal and stored under vacuum over Na/K.

Starting Materials: [(Trimethylsilyl)methyl]lithium was purchased as a 1 M solution in pentane from Aldrich, was crystallized from solution at –30 °C, and was isolated as a white crystalline solid. All other alkyllithium and Gignard reagents were purchased from Aldrich and used as received. The preparations of **1** and [$(C_5H_5)_2$Fe][BARF] have been previously reported.[8]

Instrumentation: ^{1}H NMR spectra were recorded on a Bruker DRX-400 spectrometer and were referenced to the residual protons of the solvent ([D_8]THF, 1.73 and 3.58 ppm; C_6D_6, 7.15 ppm). FTIR spectra were recorded on a Mattson Alpha Centauri spectrometer with a resolution of 4 cm^{-1}. UV/Vis spectra were recorded on a Hewlett–Packard 8453 spectrophotometer. Mass spectroscopic data were collected at the University of Delaware Mass Spectrometry Facility in electron ionization mode (+15 eV), however no chromium containing fragments were detected for any of the complexes. Elemental analyses were performed by Desert Analytics. Room-temperature magnetic susceptibility measurements were carried out using a Johnson Matthey magnetic susceptibility balance. Molar magnetic susceptibilities were corrected for diamagnetism using Pascal constants.

[Li(THF)$_4$][(^{H}L^{iPr})Cr(CH$_2$SiMe$_3$)$_2$] (2): Complex **1** (0.150 g, 0.162 mmol) was dissolved in THF (15 mL) and cooled to –30 °C. $LiCH_2SiMe_3$ (0.061 g, 0.649 mmol) was then added and the solution was stirred at room temp. for 2 h. The THF was removed, and the residue was washed with pentane and extracted into Et_2O. The Et_2O was then removed to give analytically pure **2** in 72% yield (0.209 g). Green crystalline samples of **2** can be prepared by cooling a concentrated solution to –30 °C overnight. M.p. 110 °C (decomp.). ^{1}H NMR ([D_8]THF): δ = 15.5 (2 H, aromatic), 4.70 (24 H, *i*Pr), –13.2 (4 H, *i*Pr) ppm. IR (KBr disc): $\tilde{\nu}$ = 3050 (m), 2955 (s), 2928 (s), 2881 (s), 1460 (s), 1435 (s), 1380 (m), 1318 (m), 1250 (m), 1042 (m), 888 (w), 858 (m), 759 (m) cm^{-1}. UV/Vis (THF): λ_{max} (ε, M^{-1}cm^{-1}) = 467 (3674), 569 (2972), 741 (4560) nm. μ_{eff} (294 K) = 3.7(1) μ_B. Elemental analysis consistently gave values that were significantly low in carbon and hydrogen and high in nitrogen. The exact cause is unknown, but could be due to incomplete combustion of the cation/anion pair. Cation exchange with Et_4NCl led to poor solubility causing difficulty in separating the product from LiCl.

[Li(THF)$_2$][(^{H}L^{iPr})Cr(Ph)$_2$] (3b): A sample of **1** (0.195 g, 0.210 mmol) in THF (15 mL) was cooled to –30 °C. 1.8 M LiPh (0.44 mL) was added and the solution warmed to room temp. and stirred for 2 h. The resulting solution was stripped of THF, washed with pentane, and extracted into Et_2O. The ether solution was concentrated and cooled to –30 °C to give brown **3** in 56% yield (0.173 g). M.p. 184 °C (decomp.). ^{1}H NMR ([D_8]THF): δ = 17.0 (16 H, THF), 9.42 (2 H, aromatic), 6.54 (4 H, *i*Pr), 4.34 (24 H, *i*Pr) ppm. IR (KBr disc): $\tilde{\nu}$ = 3042 (m), 3033 (m), 2957 (s), 2925 (s), 2865 (s), 1464 (s), 1432 (s), 1382 (m), 1358 (s), 1318 (m), 1246 (m), 1197 (m), 1109 (w), 1039 (s), 887 (w), 759 (m), 730 (m), 708 (s) cm^{-1}. $C_{46}H_{62}CrLiN_2O_2$ (733.94): calcd. C 75.28, H 8.51, N 3.82; found C 75.36, H 8.38, N 3.50. UV/Vis (THF) λ_{max} (ε, M^{-1}cm^{-1}) = 477 (1007), 557 (841), 871 (450) nm. μ_{eff} (294 K) = 3.7(1) μ_B.

[Li(THF)$_4$][{(^{H}L^{iPr})Cr}$_2$(μ-Me)$_3$] (4): Compound **1** (0.223 g, 0.241 mmol) was placed in THF and cooled to –30 °C. A solution of LiMe (1.6 M, 0.45 mL) was added and the solution was stirred for 2 h at room temp. The solvent was removed from the blue solution, then it was washed with pentane and extracted into Et_2O. The solution was then concentrated and cooled to –30 °C overnight to yield **4** (0.182 g, 63%) as dark blue crystals. M.p. 184 °C (decomp.). ^{1}H NMR ([D_8]THF): δ = 7.47 (2 H, aromatic), 5.50 (4 H, *i*Pr), 1.19 (12 H, *i*Pr), 0.92 (12 H, *i*Pr) ppm. IR (KBr disc): $\tilde{\nu}$ = 3052 (w), 2959 (s), 2925 (m), 2865 (m), 1460 (m), 1437 (m), 1380 (m), 1359 (w), 1320 (m), 1253 (m), 1212 (w), 1105 (w), 1042 (m), 886 (w), 799 (w), 758 (m) cm^{-1}. $C_{71}H_{117}Cr_2LiN_4O_4$ (1201.65): calcd. C 70.97, H 9.81, N 4.66; found C 70.67, H 9.68, N 4.58. UV/Vis (THF): λ_{max} (ε, M^{-1}cm^{-1}) = 491 (3528), 631 (4737), 882 (3683) nm. μ_{eff} (294 K) = 1.4(1) μ_B per Cr.

[Li(THF)$_4$][{(^{H}L^{iPr})Cr}$_2$(μ-H)$_3$] (5): A solution of **1** (0.112 g, 0.121 mmol) in THF was cooled to –30 °C and a solution of $LiBEt_3H$ (0.36 mL, 1.0 M) was added to it. The solution was allowed to stir for 2 h at room temp. resulting in a violet solution. The THF was then removed, the residue was washed with pentane and extracted into Et_2O. The solution was then concentrated and cooled to –30 °C overnight to yield **5** (0.107 g, 77%) as dark violet crystals. M.p. 164 °C (decomp.).^{1}H NMR ([D_8]THF): δ = 7.76 (2 H, aromatic), 4.07 (4 H, *i*Pr), 1.88 (24 H, *i*Pr) ppm. IR (KBr disc): $\tilde{\nu}$ = 3048 (w), 2954 (s), 2928 (m), 2861 (m), 1460 (m), 1438 (m), 1375 (m), 1347 (w), 1320 (m), 1254 (m), 1210 (w), 1107 (w), 1080 (m), 1053 (m), 1037 (m), 756 (m) cm^{-1}. $C_{60}H_{95}Cr_2N_5$ {after [Li(THF)$_4$]$^+$ for [Et$_4$N]$^+$ exchange} (990.43): calcd. C 72.76, H 9.67, N 7.07; found C 72.31, H 9.59, N 7.28. UV/Vis (THF): λ_{max} (ε, M^{-1}cm^{-1})]: 490 (4332), 631 (3931), 816 (4042) nm. μ_{eff} (294 K) = 1.5(1) μ_B per Cr.

[Li$_2$(THF)$_3$][(^{H}L^{iPr})CrMe$_3$] (6): A solution of LiMe (1.6 M, 0.83 mL) was added to a –30 °C solution of **1** (0.176 g, 0.190 mmol) in THF (10 mL). The resulting red solution was allowed to stir at room temp. for 1 h. The solvent was then removed and the crude material was dissolved in Et_2O and filtered. The Et_2O was removed and the crude red material was dissolved in pentane and crystallized overnight at –30 °C to give a 81% yield of **6** (0.267 g) as red needles. M.p. 121 °C (decomp.). ^{1}H NMR ([D_8]THF): δ = 9.12 (8 H, THF), 3.91 (24 H, *i*Pr), 2.71 (8 H, THF) ppm. IR (KBr disc):

$\tilde{\nu}$ = 3048 (w), 2958 (s), 2928 (m), 2864 (m), 1458 (m), 1435 (s), 1379 (w), 1353 (m), 1315 (m), 1248 (s), 1202 (m), 1104 (m), 1076 (m), 1041 (s), 890 (w), 759 (m) cm^{-1}. UV/Vis (THF): λ_{max} (ε, $M^{-1}cm^{-1}$) = 517 (928), 669 (334), 845 (449) nm. μ_{eff} (294 K) = 3.8(1) μ_B. Elemental analysis consistently resulted in values that were low in carbon and hydrogen content and high in nitrogen content. Upon cation exchange with an excess amount of Et_4NCl in THF, the solution turned blue and the anion of complex **4** was identified as the only product by ^1H NMR spectroscopy.

[($^{H}L^{iPr}$)Cr(CH_2SiMe_3)(THF)] (7): Compounds **1** (0.067 g, 0.072 mmol) and **2** (0.130 g, 0.145 mmol) were added to pentane (20 mL). The slurry was allowed to stir at room temp. overnight. The solvent was then removed and the residue was extracted with pentane, concentrated, and cooled to –30 °C overnight to give green **7** (0.169 g, 59% yield). M.p. 116 °C (decomp.).^1H NMR ([D_8]THF): δ = 19.5 (2 H, aromatic), 11.6 (9 H, $SiMe_3$), 2.15 (24 H, THF), –23.2 (4 H, *i*Pr) ppm. IR (KBr disc): $\tilde{\nu}$ = 3054 (w), 2957 (s), 2928 (s), 2865 (m), 1456 (m), 1439 (s), 1383 (w), 1360 (w), 1320 (m), 1254 (s), 1222 (w), 1102 (w), 860 (m), 800 (w), 757 (s) cm^{-1}. $C_{34}H_{55}CrN_2OSi$ (587.90): calcd. C 69.46, H 9.43, N 4.77; found C 69.56, H 9.59, N 5.05. UV/Vis (THF): λ_{max} (ε, $M^{-1}cm^{-1}$) = 499 (2672), 643 (2835) nm. μ_{eff} (294 K) = 3.8(1) μ_B.

[{($^{H}L^{iPr}$)Cr(μ-Me)}$_2$] (8): Pentane (25 mL) was added to **6** (0.155 g, 0.220 mmol) and **1** (0.208 g, 0.224 mmol). The slurry was allowed to stir at room temp. overnight. The solvent was removed from the resulting green solution and extracted with pentane, concentrated, and cooled to –30 °C overnight to give **8** (0.152 g, 52% yield). M.p. 162 °C (decomp.). ^1H NMR ([D_8]THF): δ = 14.4 (2 H, aromatic), 2.69 (24 H, *i*Pr), –1.91 (4 H, *i*Pr), –13.1 (6 H, CH_3) ppm. ^1H NMR (C_6D_6): δ = 17.2 (6 H, CH_3), 8.49 (2 H, aromatic), 3.88 (4 H, *i*Pr), 1.64 (24 H, *i*Pr) ppm. IR (KBr disc): $\tilde{\nu}$ = 3059 (w), 2959 (s), 2925 (m), 2866 (w), 1460 (m), 1441 (s), 1422 (m), 1383 (w), 1361 (w), 1323 (m), 1260 (s), 1222 (w), 1100 (w), 798 (w), 758 (s) cm^{-1}. $C_{59}H_{90}Cr_2N_4$ (959.37): calcd. C 73.87, H 9.46, N 5.84; found C 73.23, H 9.06, N 5.85. UV/Vis (pentane): λ_{max} (ε, $M^{-1}cm^{-1}$) = 491 (3421), 615 (1048) nm. μ_{eff} (294 K) = 1.8(1) μ_B per Cr.

[(^{H,TMSM}L*)Cr(THF)(Et_2O)][BARF] (9): Compound **7** (0.113 g, 0.192 mmol) was placed in Et_2O (20 mL). To this was slowly added a solution of [(C_5H_5)$_2$Fe][BARF] (0.200 g, 0.191 mmol) in Et_2O (10 mL). The solution was stirred for 2 h, then the Et_2O was removed, the residue was washed with pentane to remove ferrocene, then crystallized from Et_2O at –30 °C overnight to give **9** (0.120 g, 41% yield). M.p. 112 °C (decomp.). ^1H NMR ([D_8]THF): δ = 22.4 (2 H, aromatic), 7.69 (8 H, BARF), 7.49 (4 H, BARF), 3.76 (24 H, *i*Pr), –5.25 (9 H, $SiMe_3$), –23.1 (4 H, *i*Pr) ppm. IR (KBr disc): $\tilde{\nu}$ = 3071 (w), 2968 (m), 2932 (m), 2874 (m), 1610 (m), 1462 (m), 1440 (m), 1356 (s), 1277 (s), 1136 (s), 887 (m), 840 (s), 801 (w), 714 (m), 682 (m), 670 (m) cm^{-1}. $C_{70}H_{76}BCrF_{24}N_2O_2Si$ (1524.23): calcd. C 55.16, H 5.03, N 1.84; found C 55.01, H 4.86, N 2.00. UV/Vis (Et_2O): λ_{max} (ε, $M^{-1}cm^{-1}$) = 496 (748), 614 (350) nm. μ_{eff} (294 K) = 4.0(1) μ_B.

[(^{H,Me}L*)Cr(THF)$_2$][BARF] (10): Compound **8** (0.011 g, 0.012 mmol) and [(C_5H_5)$_2$Fe][BARF] (0.024 g, 0.024 mmol) were placed in a J. Young NMR spectroscopy tube followed by addition of [D_8]THF. The tube was then closed and a ^1H NMR spectrum was recorded. ^1H NMR ([D_8]THF): δ = 22.2 (2 H, aromatic), 7.78 (8 H, BARF), 7.57 (4 H, BARF), –0.41 (24 H, *i*Pr), –22.9 (4 H, *i*Pr) ppm.

Crystallographic Structure Determinations: A summary of the crystal data collection and refinement parameters for compounds **2**–**9** can be found in the Supporting Information. Suitable crystals were selected, mounted with viscous oil, and cooled to 120 K. Data were collected on a Bruker APEX CCD diffractometer using graphite-monochromated Mo-K_α radiation (λ = 0.71073 Å). Unit-cell parameters were obtained from three sets of 20 frames using 0.3° ω scans from different sections of the Ewald sphere. Data sets were corrected for absorption using SADABS multiscan methods.[18] No symmetry higher than triclinic was observed for complexes **5** and **9**. Systematic absences in the diffraction data and unit-cell parameters are consistent with $P2_1/n$ (=$P2_1/c$; no. 14), uniquely, for complexes **2**, **7**, **3**, and **4**; and, *Cc* (no. 9) and *C*2/*c* (no. 15) for complexes **6** and **8**. The centrosymmetric space group options yielded chemically reasonable and computationally stable results of refinement. Structures were solved by direct methods and refined with full-matrix least-squares methods based on F^2. Two symmetry unique but chemically similar molecules are located in the asymmetric unit for complex **7**. The compound molecule is located at a twofold axis in **8**. Four structures display cocrystallized solvent molecules: **2** (0.5 Et_2O); **5** (Et_2O); **8** (0.5 pentane); and **9** (pentane), each per asymmetric unit. Solvent molecules in **8** and **9** were treated as diffused contributions using Squeeze.[19] All non-hydrogen atoms were refined anistropically. All hydrogen atoms were treated as idealized contributions except for the bridging hydrides in **5**, the bridging methyl protons in **4**, **6**, and **7**, and the hydrogen atoms of the methylene C30 in **9**, which were located in difference maps. Located hydrogen atoms were positionally refined but with isotropic parameters constrained to 1.2U_{eq} of the attached carbon atom for the methyl and methylene groups, and of the chromium atoms for the hydrides. All atomic scattering factors are included in the SHELXTL program library.[18]

CCDC-837092 (for **2**), -837093 (for **3**), -837094 (for **4**), -837095 (for **5**), -837096 (for **6**), -837097 (for **7**), -837098 (for **8**), and -837099 (for **9**) contain the supplementary crystallographic data for this paper. These data can be obtained free of charge from The Cambridge Crystallographic Data Centre via www.ccdc.cam.ac.uk/data_request/cif.

Supporting Information (see footnote on the first page of this article): X-ray crystallographic data for complexes **2**–**9**, the details of the DFT calculations of **7′**, **7′′**, **8′**, and **8′′** and the complete citation for the Gaussian 03 software package.

Acknowledgments

We thank the University of Wisconsin-Madison's Chemistry Computer Center for computational assistance. This research was supported by grants from the Nation Science Foundation (NSF) (to K. H. T., grant numbers CHE-0616375 and CHE-0911081).

[1] a) P. J. Chirik, K. Wieghardt, *Science* **2010**, *327*, 794–795; b) D. Astruc, C. Ornelas, J. Ruiz, *Acc. Chem. Res.* **2008**, *41*, 841–856; c) J. L. Boyer, J. Rochford, M. K. Tsai, J. T. Muckerman, E. Fujita, *Coord. Chem. Rev.* **2010**, *254*, 309–330; d) A. K. Das, B. Sarkar, J. Fiedler, S. Zalis, I. Hartenbach, S. Strobel, G. K. Lahiri, W. Kaim, *J. Am. Chem. Soc.* **2009**, *131*, 8895–8902; e) A. Dei, D. Gatteschi, C. Sangregorio, L. Sorace, *Acc. Chem. Res.* **2004**, *37*, 827–835; f) A. Diez, E. Lalinde, M. T. Moreno, S. Sanchez, *Dalton Trans.* **2009**, 3434–3446; g) E. Evangelio, D. Ruiz-Molina, *Eur. J. Inorg. Chem.* **2005**, 2957–2971; h) S. I. Gorelsky, A. B. P. Lever, M. Ebadi, *Coord. Chem. Rev.* **2002**, *230*, 97–105; i) A. B. P. Lever, S. I. Gorelsky, *Struct. and Bonding* **2004**, *107*, 77–114; j) K. A. McNitt, K. Parimal, A. I. Share, A. C. Fahrenbach, E. H. Witlicki, M. Pink, D. K. Bediako, C. L. Plaisier, N. Le, L. P. Heeringa, D. A. V. Griend, A. H. Flood, *J. Am. Chem. Soc.* **2009**, *131*, 1305–1313; k) E. L. Rosen, C. D. Varnado, A. G. Tennyson, D. M. Khramov, J. W.

Kamplain, D. H. Sung, P. T. Cresswell, V. M. Lynch, C. W. Bielawski, *Organometallics* **2009**, *28*, 6695–6706; l) P. Zanello, M. Corsini, *Coord. Chem. Rev.* **2006**, *250*, 2000–2022.
[2] a) S. C. Bart, K. Chlopek, E. Bill, M. W. Bouwkamp, E. Lobkovsky, F. Neese, K. Wieghardt, P. J. Chirik, *J. Am. Chem. Soc.* **2006**, *128*, 13901–13912; b) C. C. Lu, E. Bill, T. Weyhermuller, E. Bothe, K. Wieghardt, *J. Am. Chem. Soc.* **2008**, *130*, 3181–3197.
[3] a) N. Muresan, K. Chlopek, T. Weyhermüller, F. Neese, K. Wieghardt, *Inorg. Chem.* **2007**, *46*, 5327–5337; b) N. Muresan, T. Weyhermüller, K. Wieghardt, *Dalton Trans.* **2007**, 4390–4398; c) M. Ghosh, T. Weyhermüller, K. Wieghardt, *Dalton Trans.* **2008**, 5149–5151; d) M. Ghosh, S. Sproules, T. Weyhermüller, K. Wieghardt, *Inorg. Chem.* **2008**, *47*, 5963–5970; e) N. Muresan, C. C. Lu, M. Ghosh, J. C. Peters, M. Abe, L. M. Henling, T. Weyhermüller, E. Bill, K. Wieghardt, *Inorg. Chem.* **2008**, *47*, 4579–4590; f) M. M. Khusniyarov, T. Weyhermüller, E. Bill, K. Wieghardt, *J. Am. Chem. Soc.* **2009**, *131*, 1208–1221.
[4] G. Vankoten, K. Vrieze, *Adv. Organomet. Chem.* **1982**, *21*, 151–239.
[5] a) E. Wissing, S. Vanderlinden, E. Rijnberg, J. Boersma, W. J. J. Smeets, A. L. Spek, G. Vankoten, *Organometallics* **1994**, *13*, 2602–2608; b) M. Kaupp, H. Stoll, H. Preuss, W. Kaim, T. Stahl, G. Vankoten, E. Wissing, W. J. J. Smeets, A. L. Spek, *J. Am. Chem. Soc.* **1991**, *113*, 5606–5618; c) E. Wissing, E. Rijnberg, P. A. Vanderschaaf, K. Vangorp, J. Boersma, G. van Koten, *Organometallics* **1994**, *13*, 2609–2615; d) E. Wissing, M. Kaupp, J. Boersma, A. L. Spek, G. Vankoten, *Organometallics* **1994**, *13*, 2349–2356; e) E. Rijnberg, J. Boersma, J. Jastrzebski, M. T. Lakin, A. L. Spek, G. vanKoten, *Organometallics* **1997**, *16*, 3158–3164; f) E. Rijnberg, B. Richter, K. H. Thiele, J. Boersma, N. Veldman, A. L. Spek, G. van Koten, *Inorg. Chem.* **1998**, *37*, 56–63.
[6] a) P. J. Bailey, R. A. Coxall, C. M. Dick, S. Fabre, S. Parsons, L. J. Yellowlees, *Chem. Commun.* **2005**, 4563–4565; b) P. J. Bailey, C. M. Dick, S. Fabre, S. Parsons, L. J. Yellowlees, *Dalton Trans.* **2006**, 1602–1610; c) M. G. Gardiner, G. R. Hanson, M. J. Henderson, F. C. Lee, C. L. Raston, *Inorg. Chem.* **1994**, *33*, 2456–2461.
[7] a) P. De Waele, B. A. Jazdzewski, J. Klosin, R. E. Murray, C. N. Theriault, P. C. Vosejpka, J. L. Petersen, *Organometallics* **2007**, *26*, 3896–3899; b) R. D. J. Froese, B. A. Jazdzewski, J. Klosin, R. L. Kuhlman, C. N. Theriault, D. M. Welsh, K. A. Abboud, *Organometallics* **2011**, *30*, 251–262; c) H. Tsurugi, R. Ohnishi, H. Kaneko, T. K. Panda, K. Mashima, *Organometallics* **2009**, *28*, 680–687; d) H. Kaneko, H. Tsurugi, T. K. Panda, K. Mashima, *Organometallics* **2010**, *29*, 3463–3466; e) K. Mashima, R. Ohnishi, T. Yamagata, H. Tsurugi, *Chem. Lett.* **2007**, *36*, 1420–1421.
[8] K. A. Kreisel, G. P. A. Yap, K. H. Theopold, *Inorg. Chem.* **2008**, *47*, 5293–5303.
[9] a) J. P. Hogan, *J. Polym. Sci. Polym. Chem. Ed.* **1970**, *8*, 2637–2652; b) E. Groppo, C. Lamberti, S. Bordiga, G. Spoto, A. Zecchina, *Chem. Rev.* **2005**, *105*, 115–183.
[10] L. A. MacAdams, G. P. Buffone, C. D. Incarvito, A. L. Rheingold, K. H. Theopold, *J. Am. Chem. Soc.* **2005**, *127*, 1082–1083.
[11] R. L. Carlin, *Magnetochemistry*, Springer, Berlin, **1986**.
[12] C. Janiak, J. Silvestre, K. H. Theopold, *Chem. Ber.* **1993**, *126*, 631–643.
[13] R. Bau, M. H. Drabnis, *Inorg. Chim. Acta* **1997**, *259*, 27–50.
[14] a) R. A. Heintz, B. S. Haggerty, H. Wan, A. L. Rheingold, K. H. Theopold, *Angew. Chem.* **1993**, *105*, 1136; *Angew. Chem. Int. Ed. Engl.* **1992**, *31*, 1077–1079; b) R. A. Heintz, B. S. Haggerty, H. Wan, A. L. Rheingold, K. H. Theopold, *Angew. Chem.* **1992**, *104*, 1100; *Angew. Chem. Int. Ed. Engl.* **1992**, *31*, 1077–1079; c) R. A. Heintz, T. F. Koetzle, R. L. Ostrander, A. L. Rheingold, K. H. Theopold, P. Wu, *Nature* **1995**, *378*, 359–362; d) R. A. Heintz, R. L. Ostrander, A. L. Rheingold, K. H. Theopold, *J. Am. Chem. Soc.* **1994**, *116*, 11387–11396.
[15] X. J. Yang, J. Yu, Y. Y. Liu, Y. M. Xie, H. F. Schaefer, Y. M. Liang, B. Wu, *Chem. Commun.* **2007**, 2363–2365.
[16] K. A. Kreisel, G. P. A. Yap, O. Dmitrenko, C. R. Landis, K. H. Theopold, *J. Am. Chem. Soc.* **2007**, *129*, 14162–14163.
[17] S. D. Ittel, L. K. Johnson, M. Brookhart, *Chem. Rev.* **2000**, *100*, 1169–1203.
[18] G. M. Sheldrick, *Acta Crystallogr., Sect. A* **2008**, *64*, 112–122.
[19] A. L. Spek, *J. Appl. Crystallogr.* **2003**, *36*, 7–13.

Received: August 1, 2011
Published Online: September 27, 2011

